Characterization of polypropylene pulsating heat stripes: effects of orientation, heat transfer fluid, and loop geometry

Oguzhan Der, Ali Ahmed Alqahtani[1]

Laboratory of Technical Physics, University of Liverpool, Brownlow Hill, Liverpool L69 3GH, United Kingdom

Marco Marengo

School of Computing, Engineering and Mathematics, University of Brighton, Lewes Road, Brighton BN2 4GJ, United Kingdom

Volfango Bertola[*]

Laboratory of Technical Physics, University of Liverpool, Brownlow Hill, Liverpool L69 3GH, United Kingdom

Abstract

A parametric analysis of the thermal performance of flat polypropylene pulsating heat pipes (PHPs) is presented. In particular, the thermal performance was characterized for pulsating heat pipes with different number of turns of the serpentine channel, different orientations with respect to gravity, and containing different heat transfer fluids. The dependence of polymeric PHPs performance on design parameters is poorly understood to date. The development of polymeric PHPs characterized by high mechanical flexibility will have significant impact on thermal management of smartphones, portable electronics, and deployable systems such as cube satellites. Several prototype PHPs with different number of turns of the serpentine channel were fabricated bonding together three polypropylene sheets by selective transmission laser welding, after cutting out a serpentine channel in the central sheet. The thermal performance of the devices was characterized by supplying an ascending/descending stepped thermal power ramp to the evaporator, and measuring the corresponding equivalent thermal resistance between the evaporator and the condenser.

Keywords: Pulsating heat pipes, Plastic heat pipe, Selective transmission laser welding

[*]Corresponding author

Email address: `Volfango.Bertola@liverpool.ac.uk` (Volfango Bertola)

[1]Permanent address: Mechanical Engineering Department, College of Engineering, King Khalid University, Abha 61413 Asir, Saudi Arabia.

1. Introduction

The increasing technology challenges posed by volumetric density scaling in smart systems integration and functional electronic packaging [1] drive the interest in high-performace, compact heat transfer devices for thermal management of computers, data centres, smartphones, high power electronics, and cooling boards. In this context, passive two-phase capillary driven loops, such as pulsating heat pipes (PHPs) are a very promising, simple and cost effective technology compared to other heat transport devices [2, 3].

A pulsating heat pipe consists of a small diameter tube arranged in a serpentine or multi-turn structure and evacuated to a high-vacuum level (10^{-3} mBar). A heat transfer fluid free from non-condensable gases and with thermo-physical properties suitable to maximize the heat transfer is then fed to the system, only partially filling the device. Once the PHP is sealed, the heat transfer fluid circulates alternating liquid slugs and vapour plugs due to the dominant effect of capillary forces with respect to the buoyancy forces. The fluid motion as well as the flow pattern transitions are rather chaotic, however the system is able to reach a pseudo-steady state over a wide range of operating conditions [4]. The pressure fluctuations inside the PHP drive a self-excited oscillating motion of liquid plugs and vapour bubbles [5], significantly enhancing convection and consequently promoting the heat transfer of both sensible and latent heat between a thermal source (evaporator) and a thermal sink (condenser) [6]. The advantages of PHPs with respect to standard heat transfer technologies, such as purely conductive systems or single phase forced loops, are mainly related to the exploitation of the high heat transfer rates associated with the phase change phenomenon, the compactness and the possibility to be operated passively, avoiding the use of pumps and gravity.

To address the demand of heat transfer devices characterized by low weight, small unit thickness, low cost, and high mechanical flexibility, it was recently proposed to embed the PHP serpentine channel into a composite polypropylene sheet [7, 8]. The concept is to cut out the serpentine channel in a black polypropylene sheet, sandwiched between two transparent sheets of the same material and bonded together by selective transmission laser welding [9, 10]. Due to the small thickness of the polymer sheet, the PHP channel has a large aspect ratio, resulting into so-called "pulsating heat stripes" (PHS), which can be seen in practice as an engineered composite polymer sheet with enhanced thermal conductivity [11, 12]. The development of polymeric PHPs charachterized by high mechanical flexibility will have significant impact on thermal management of smartphones, portable electronics, and deployable systems such as cube satellites.

The liquid and gas diffusion through the polymer and the billowing of the flexible material due to pressure differentials are two important technical issues affecting pulsating heat pipes built with polymeric materials. Very recently, a

2

flexible pulsating heat pipe was fabricated by thermally sintering a multilayer polymer film including an aluminum layer acting as gas barrier on the two sides of a low-density polyethylene sheet cut into a closed-loop PHP shape [13]. To minimize diffusion of noncondensable gases through the seal, an indium coating was deposited on the heat pipe perimeter.

The list of parameters influencing the PHP effectiveness is quite long, the most important ones being the heat transfer fluid, the applied heat flux, the filling ratio, the two-phase flow distribution, the liquid film thickness, the characteristics of the fluid oscillations, the gravity level, and the geometrical features, just to mention the most relevant ones [14, 15]. Whilst there seems to be a wide consensus on the optimal value of the filling ratio (50-60%), the effect of many other parameters is poorly understood or strongly case-dependent. The PHP geometrical parameters impact in complex way on the PHP behaviour. The overall length of the channel, the number of turns, the evaporation, adiabatic and condenser section lengths, the radius of the channel turns, have rather intricate and not well understood effects on the PHP behaviour. Furthermore, increasing the number of turns improves the operation stability, and allows to dissipate higher power inputs with almost comparable evaporator temperatures, resulting into a decrease of the thermal resistance.

Because the development of polymeric pulsating heat pipes is still in its infancy, to date there is no systematic assessment of the effect of design parameters on their performance. To partially address this gap in the current understanding of polymeric pulsating heat pipes, the present work reports the results of an experimental investigation of the effects of orientation, heat transfer fluid and loop geometry on the thermal performance of a flat polypropylene pulsating heat pipe.

2. PHS design

The pulsating heat pipes (or PHS) used in the present study were fabricated using rectangular polypropylene sheets (average thermal conductivity: 0.16 W/mK) having a length of 250 mm and a width of 100 mm. First, the serpentine channel was cut-out in a black sheet (0.7 mm thickness) using a commercial laser cutter (HPC Laser LS1290 Pro). Then, the channel was sandwiched between two transparent sheets (0.4 mm thickness each), which were tightly bonded to the black sheet by selective transmission laser welding using a nanosecond pulsed fibre laser (SPI Lasers G4 HS-L 20W) [7, 8, 11, 12]. The resulting composite polypropylene sheet had an overall thickness of 1.5 mm.

The most important design parameters of a pulsating heat pipe are the hydraulic diameter, $D_H = 2Wt/(W + t)$, where W is the channel width and t its height, and the number of turns of the serpentine channel. To ensure the fluid circulation is driven by capillary forces instead of buoyancy, one must set an upper limit to the Bond number

$$Bo = \frac{g(\rho_l - \rho_v)D_H^2}{\sigma} \tag{1}$$

3

Table 1: Fluid properties at ambient temperature and at saturation temperature.

	T [°C]	ρ_l [kg/m^3]	ρ_v [kg/m^3]	H_{lv} [kJ/kgK]	σ [mN/m]	η [mPa·s]	θ [°]	P_v [kPa]
water	20	998	0.008	2453	72	1	85	2.34
water	99	959	0.6	2256	59	0.28	55	101
ethanol	20	789	0.145	919	24	1.18	≈ 0	5.83
ethanol	78	737	1.87	846	17	0.45	≈ 0	100
FC-72	20	1688	3.46	95	12.7	0.64	≈ 0	27
FC-72	56	1594	13.1	88	7.8	0.43	≈ 0	100

where g is gravity, ρ_l and ρ_v are, respectively, the liquid and the vapour densities, and σ is the surface tension. Studies of capillary flow [16] and flooding in vertical up-flow [17] and of heat transfer in confined spaces under a variety of conditions [18, 19, 20] suggest that capillary effects are significant for channels having hydraulic diameters such that the $Bo < 4$ [21, 22]. There is also experimental evidence of a lower limit for PHP operation, $Bo > 0.4$ [23]. This results into the following lower and upper limits for the hydraulic diameter:

$$0.63\sqrt{\frac{\sigma}{g(\rho_l - \rho_v)}} \leq D_H \leq 2\sqrt{\frac{\sigma}{g(\rho_l - \rho_v)}} \tag{2}$$

According to Eq. (2), the range of acceptable hydraulic diameters depends only of the fluid properties, which in turn depend on temperature. In the present work, three commonly used heat transfer fluids (water, ethanol, and perfluorohexane FC-72) were considered, and their properties are listed in Table 1. All properties were taken from the reference literature, except the contact angle, which was measured from side view images of liquid drops deposited on the same polyropylene sheets used to fabricate the PHP using a specific digital image processing method [24, 25].

Because one dimension of the channel cross-section is fixed ($t = 0.7$ mm), the hydraulic diameter and the Bond number for a given fluid depend only on the channel width. Figure 1a displays the Bond number as a function of the channel width, for the three fluids considered, with thermophysical properties evaluated at ambient temperature (20°C) and at the boiling point, i.e. the limits of the temperature range where the fluid is in the liquid state. This figure shows that in the case of FC-72 and ethanol, the Bond number falls within the range suitable to PHP operation for channel widths between 2.5 and 10 mm, while the Bond numbers relative to water are too low for PHP operation, for any channel width.

The upper and lower limits on the Bond number (Eq. 1), and consequently those on the hydraulic diameter (Eq. 2), however, were determined based on experiments in metallic or glass capillary tubes, where the liquid is in contact with materials characterised by high surface energy hence high wettability [26]. In the case of polypropylene, the surface energy of the channel walls is
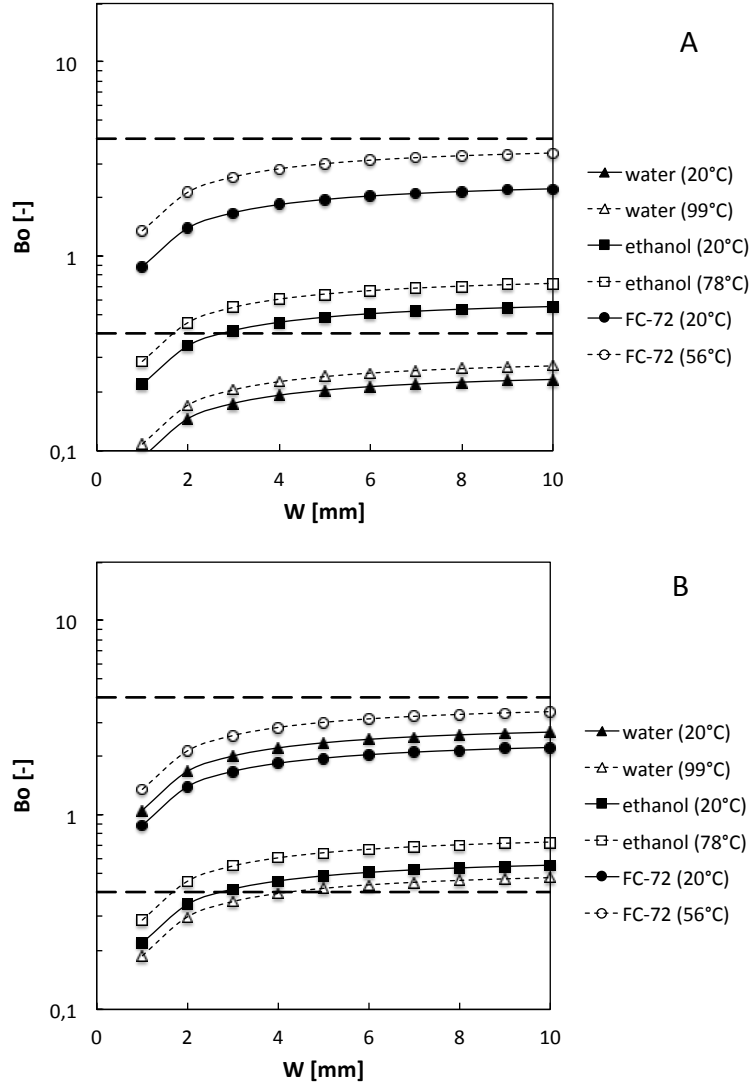
Figure 1: Bond number for water, ethanol and FC-72 at ambient temperature and at the boiling point, plotted as a function of the channel width without considering wettability (a) and including the effect of wettability (b). The long-dashed horizontal lines indicate the lower and upper limits ($Bo = 0.4$ and $Bo = 4$, respectively) on the Bond number.

significantly lower, therefore the capillary force at thermodynamic equilibrium reduces according to the Young-Laplace equation, and the Bond number should be calculated as

$$Bo = \frac{g(\rho_l - \rho_v)D_H^2}{\sigma \cos \theta} \qquad (3)$$

5

where θ is the equilibrium contact angle of the fluid on polypropylene. Accordingly, the range of acceptable hydraulic diameters for PHP operation becomes:

$$0.63\sqrt{\frac{\sigma\cos\theta}{g(\rho_l - \rho_v)}} \leq D_H \leq 2\sqrt{\frac{\sigma\cos\theta}{g(\rho_l - \rho_v)}} \tag{4}$$

Taking into account the fluid wettability (Eq. 3), the Bond numbers corresponding to the three fluids considered change as shown in Figure 1b, which suggests the Bond number falls within the range suitable to PHP operation for all of the three fluids considered. In particular, the contact angle listed in Table 1 indicate that both ethanol and FC-72 have a very high wettability on polypropylene surfaces ($\theta \approx 0°$), so that $cos\theta \approx 1$ therefore the Bond number does not change when Eq. (1) is used instead of Eq. (3). In the case of water, the contact angle is significantly higher so that the Bond number calculated using Eq. (3) is higher than the Bond number calculated using Eq. (1).
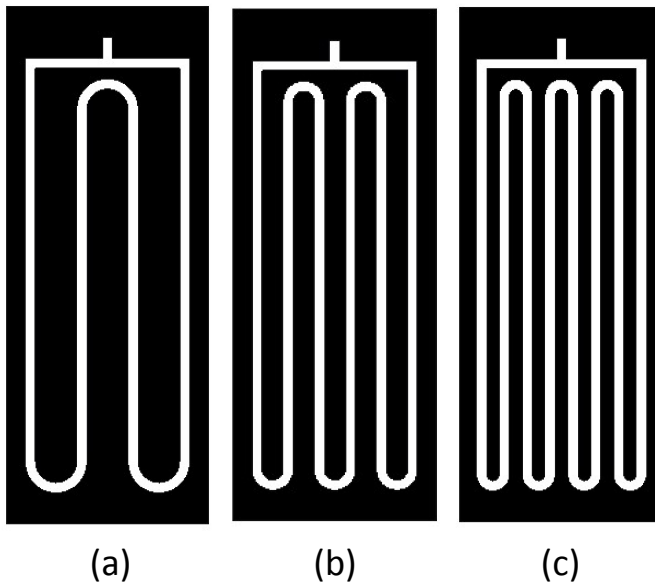

Figure 2: Prototype pulsating heat stripes with 3-turns (a), 5-turns (b), and 7-turns (c) serpentine channel.

Another constraint on the channel width is due by the relatively low elastic modulus of polypropylene. If the channel width is large, the thin (0.4 mm) polypropylene wall changes its shape according to the pressure difference between the heat transfer fluid and the atmosphere. This affects both the pressure level during operation and the hydraulic diameter, as shown by preliminary experiments conducted on a polypropylene PHP/PHS having a channel width of 9 mm [8].

6

In conclusion, a channel width $W = 5$ mm was selected to meet all of the above constraints, corresponding to a hydraulic diameter $D_H = 1.23$ mm. As for the number of turns, three pulsating heat pipe designs were produced with three, five, and seven turns, respectively, as illustrated in Figure 2. On the condenser side, the main loop is connected to a short auxiliary channel where a small hole in one of the channel walls enables fitting a valve and a pressure sensor.

3. Experimental setup and procedure

3.1. Experimental setup

Figure 3 shows the schematic layout of the experimental setup. The PHS units were mounted on a support frame, clamped in correspondence of the evaporator zone and of the condenser zone. The support frame could be inclined at any angle by means of a lab scissors jack. Each side of the evaporator clamp consisted of a rectangular plywood plate (15 cm length, 5 cm width, 1.5 cm thickness) insulated on one side by a 1 cm layer of Superwool 607HT (Thermal Ceramics Ltd.), a material with thermal conductivity ≤ 0.05 W/mK. The insulating layer was shaped to host a 100 W ceramic heater and a flush-mounted copper plate (10 cm length, 4 cm width), to distribute the heat supply uniformly on the PHP/PHS evaporator surface. Heat sink paste was used to minimise the contact resistance between the ceramic heater and the copper plate. The heaters were connected to a regulated DC power supply (Circuit Specialists CSI 12001X) to enable a fine control of the power input (instrumental accuracy: $\pm 2.2\%$).

In the condenser section, the PHS were clamped between two aluminium plates coated with a thin layer of heat sink paste; two fan-assisted heat sinks (Malico) were mounted on the external plate. The evaporator and the condenser sections had an identical length of 4 cm.

The heat pipe was connected to a pressure transducer (Gems 3500, 0-160 kPa, instrumental accuracy: ± 0.4 kPa) and to an aluminium needle valve, used in turn to vacuum the PHS and to fill the PHS with the heat transfer fluid. The valve and the pressure sensor were mounted on two orthogonal sides of a rectangular aluminium block previously drilled to create a T-junction. The aluminium block was then glued on the PHP/PHS surface so that the T-junction hole corresponded to the hole on the PHP/PHS auxiliary channel wall, and secured by two bolts passing through the solid part of the PHP/PHS and a counter-plate, as shown in Figure 4. The pressure transducer DC output was sampled at 1 Hz by a data acquisition system (LabJack U6).

Eight surface thermocouples (Omega Engineering) with response time $\leq$ 0.3 s and flat probe junction (instrumental accuracy: 0.75%) were securely fastened between the PHS surface and the clamps, four in the evaporator zone and four in the condenser zone, and connected to a data acquisition system. The temperature distribution in the adiabatic region was monitored by a FLIR infra-red camera (Hti-Xintai A1).
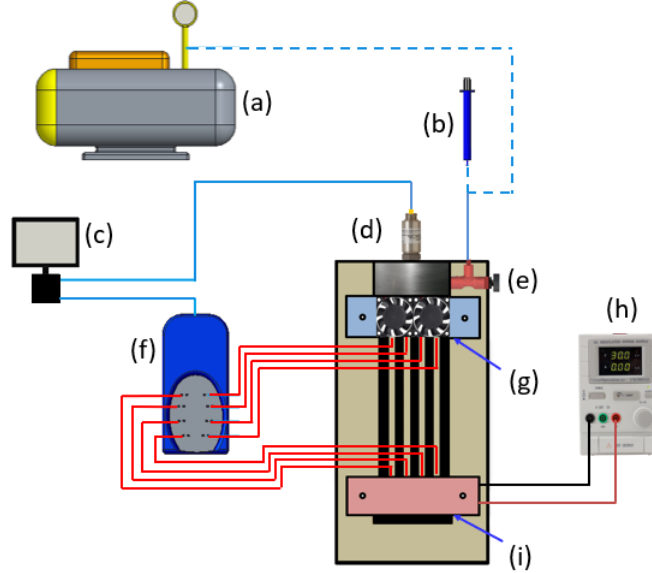
7

Figure 3: Schematic layout of the experimental setup: (a) vacuum pump, (b) syringe, (c) data logger and PC, (d) pressure transducer, (e) micro-metering valve, (f) thermocouples data logger, (g) condenser fans, (h) power supply, and (i) electric heaters.

3.2. Procedure

The heat transfer fluids used in experiments were de-gassed in a vacuum chamber (Bacoeng) for 24 hours before use. To introduce the heat transfer fluid, the PHS modules were vacuumed to a pressure of 0.5 ± 0.1 kPa (abs) using a two-stage vacuum pump (Bacoeng); then, the fluid contained in an external syringe reservoir was slowly driven by the atmospheric pressure into the PHS as the micro-metering valve was gently opened. The filling ratio was 40% of the total PHP/PHS volume (1.4 mL, 1.9 mL and 2.6 mL, respectively, for the 3-turns, 5-turns, and 7-turns PHP/PHS); the filling ratio was determined based on preliminary tests to ensure a maximum pressure of approximately 1.5 bar (abs).

Experiments were conducted by applying to the evaporator section an ascending/descending stepped power ramp ranging approximately between 4 W and 30 W, and measuring the temperatures on the PHS surface at a sampling rate of 1 Hz. The magnitude of the first step was approximately 4 W to ensure start-up, based on preliminary tests [7], while the magnitude of subsequent steps was approximately 9 W. For each power step, the heat supply was kept constant until a pseudo steady-state regime was attained, which typically required about 30 minutes. Tests were interrupted earlier in case any point of the PHS reached a temperature of 120°C, to avoid polypropylene softening and/or melting. Preliminary experiments [7] showed the start-up of two-phase circulation
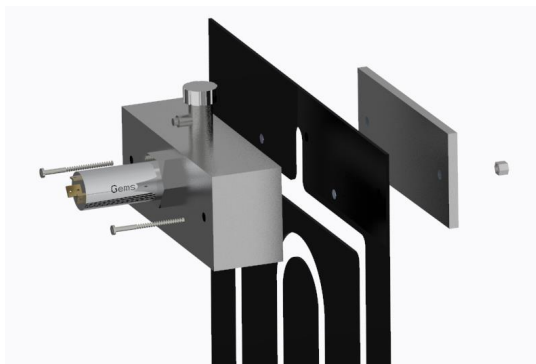
8

Figure 4: Schematic the pressure transducer and micro-metering valve assembly.

in the PHS occurs with a heat input of about 2.5 W at the evaporator.

The equivalent thermal resistance of the PHS was calculated as:

$$R = \frac{T_{ev} - T_{cond}}{\dot{Q}} \qquad (5)$$

where T_{ev} and T_{cond} are the averages of the four temperature measurements of the PHS surface at the evaporator and the condenser, respectively, in the pseudo steady-states corresponding to each level of the power input, $\dot{Q}$. The resulting instrumental error on the power input magnitude is 3.3%. For the sake of comparison with the thermal resistance of the bare composite polypropylene sheet, one test was carried out using a vaccumed PHS module, without heat transfer fluid.

For each of the channel geometries considered (see Figure 2), experiments were carried out for three PHS orientations: (i) vertical, (ii) inclined at 45°, (iii) horizontal. To ensure homogeneous experimental conditions, each test was carried out using a fresh PHS unit. However, this makes full uncertainty quantification across different samples impossible due to the complexity of the manufacturing process and of the filling procedure. In particular, small non-homogeneities in the polymer sheets may result into small variations of the channel roughness and width, as well as on the thickness and quality of the welded layer. In addition, the flexibility of the plastic walls of the PHP channels makes it extremely sensitive to small variations of the vacuum level before filling, and of the atmospheric pressure during tests. Finally, because of the small inner volume of the serpentine channel (of the order of 2 mL, depending on the number of turns) the manual filling procedure slightly affects the filling ratio.

9

4. Results and discussion

4.1. Response to a stepped power ramp

An initial qualitative visualization of the PHP/PHS response to an ascending/descending stepped power ramp supplied to the evaporator is given by FLIR images of the adiabatic region, which are displayed in Figure 5 for PHP/PHS in straight vertical arrangement and with 3-turns, 5-turns, and 7-turns serpentine channel, respectively.
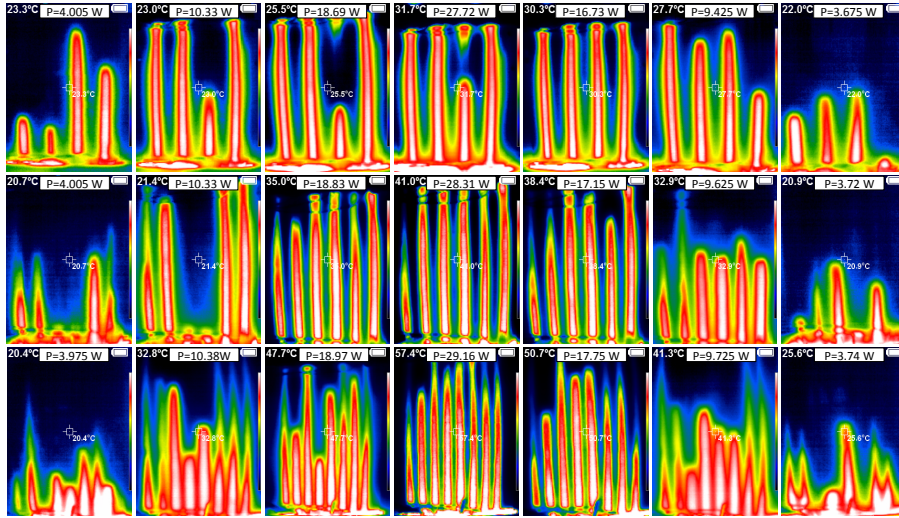

Figure 5: FLIR snapshots of the adiabatic region of a 3-turns (top), 5-turns (center), and 7-turns (bottom) PHP/PHS with vertical orientation and containing FC-72, during an ascending/descending stepped heating power ramp supplied to the evaporator.

Upon increasing the thermal power supply, one can observe the number of active (i.e., heated) sections of the serpentine channel grows, as well as the active length of each section. As the number of turns increases, there is a more uniform distribution of the thermal power on the PHP/PHS surface. When the thermal power supply is progressively decreased, both the number of active sections and their active length decrease, however the thermal inertia of the system is not negligible and induces hysteresis. In the case of the 3-turn channel, the full activation of all sections occurs during the first step of the descending ramp, long after the maximum thermal power supply has been reached.

Figure 6 shows temperatures measured in the evaporator and in the condenser zones of the 3-turns PHS during the ascending/descending heat supply ramp, for the three heat transfer fluids considered and different orientations, while the corresponding absolute pressures in the serpentine channel are displayed in Figure 7. Similar results were obtained for the 5-turns and the 7-turns PHS. In several cases, the maximum heating power could not be maintained until the system reached a pseudo-steady state because the temperature gradient

10

was too steep (Figure 6), therefore the evaporator temperature could locally approach or exceed the limit imposed by the material.
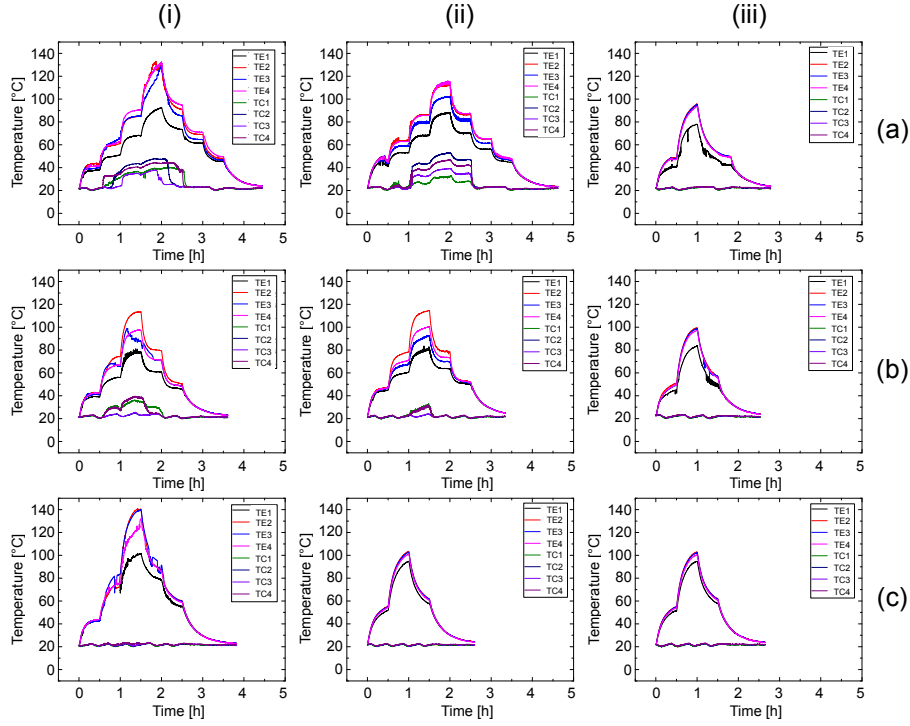

Figure 6: Temperatures measured at the evaporator and the condenser of a 3-turns PHP containing FC-72 (a), ethanol (b), water (c), with vertical (i), 45° (ii), and horizontal (iii) orientation, during an ascending/descending stepped heating power ramp supplied to the evaporator. The power levels are 4±0.5 W, 10±0.5 W, 18±0.7 W and 28±0.8 W.

At lowest heating power supply (about 4 W), corresponding to the PHP/PHS start-up [7, 8], boiling is still weak, therefore its intensity does not change significantly in the different channels. Thus, the temperature measured at different points of the evaporator zone surface is approximately uniform. As the heating power supply is increased one can observe significant differences among measurements taken in correspondence of different points of the serpentine channel, the lower temperatures being measured in correspondence of the sections of the channel with stronger fluid circulation. This happens because when the heating power supply is increased, the intensity of boiling also increases, however the intensity of boiling can be very different inside adjacent channels due to the well-known instabilities of two-phase mixtures in parallel channels [27]. Thus, in channels where boiling is stronger the heat removal from the evaporator zone is more effective than in channels where boiling is weaker, which causes the difference in the temperature measured at different points of the evaporator zone. Similar considerations apply to local temperatures measured on the surface of

11
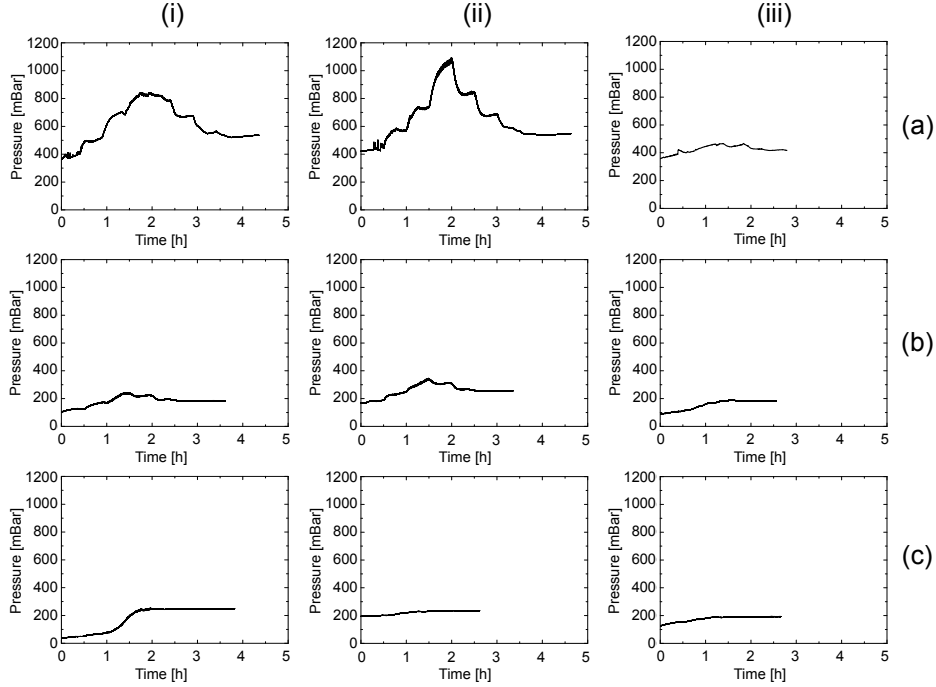
Figure 7: Pressure measured in a 3-turns PHP containing FC-72 (a), ethanol (b), water (c), with vertical (i), 45° (ii), and horizontal (iii) orientation, during an ascending/descending stepped heating power ramp supplied to the evaporator.

the condenser zone.

The main difference between the ascending and the descending power ramp is that, for the same magnitude of the heating power supply, the temperatures measured in the pseudo-steady state during the descending ramp are slightly but systematically higher than the temperatures measured during the ascending ramp. As a result, the behaviour of the device during a heating/cooling cycle shows a hysteresis, similar to most pulsating heat pipes [22].

The pressure measured inside the serpentine channel (Figure 7) qualitatively mirrors the trend observed for temperature measurements, although it displays a somewhat smoother response to step changes in the heating power supply. At the end of each test (2.5 to 5 hours), one can observe a small increase of pressure with respect to the beginning, which could be due to (i) gas permeation through the polymer channel walls, (ii) potential imperfections in manufacturing (iii) micro-leaks in the connection with the valve and the pressure sensor, (iv) the viscoelastic relaxation of the polymer channel walls [8]. Whilst this minor pressure increase does not affect significantly the device performance within the duration of a single test, it represents an obvious issue over long periods of time. However, the use of gas barrier layers such as a metallic coating was deliberately avoided both because it would prevent the visual inspection of the flow, and

12

because the purpose of the present experiments was to evaluate the thermal performance increase of the PHP/PHS in different configurations with respect to the raw polymer material. At present, there is only one study investigating the performance loss of a polymeric pulsating heat pipe due to gas permeation [13], however a direct comparison with the present results is not possible because the materials used in the two studies (low-density polyethylene and polypropylene, respectively), have different permeation coefficients.

4.2. Effect of design parameters

The performance of the PHP/PHS achieved with different combinations of the design parameters was estimated based on the values of the equivalent thermal resistance, defined by Eq. (5). Figure 8 displays the measured equivalent thermal resistance as a function of the heating power supply at the evaporator during an ascending/descending heating power ramp, for all the combinations of design parameters considered. With the exception of the horizontal PHP/PHS, the equivalent thermal resistance decreases exponentially with increasing heating power.

In the case of FC-72 and ethanol, and inclinations of 45° and vertical, the measured values of the equivalent thermal resistance are identical within the experimental error, both during the ascending and during the descending heating power supply ramps. In these cases, the PHP/PHS attain the overall minimum equivalent thermal resistance for a heating power supply of about 30 W. Its magnitude is four to five times smaller than the equivalent thermal resistance measured for the PHP/PHS envelope in the absence of heat transfer fluid (10.8 °C/W). This corresponds to a four- to five-fold increase of the PHP/PHS thermal performance compared to a composite polypropylene sheet having the same composition, size, thickness and weight, in agreement with previous results [8, 11, 12].

In the case of water, the magnitude of the equivalent thermal resistance is much closer to the value measured without heat transfer fluid, and does not exhibit a clear monotonically decreasing trend as the heating power supply is increased. This can be explained with the low saturation pressure, which requires a high vacuum in the serpentine channel, and to the large latent heat, which requires large heating power supplies hence larger temperatures at the evaporator in order to produce the amount of vapour necessary to activate the liquid-vapour mixture circulation. Since in polymeric PHP/PHS the maximum temperature at the evaporator is limited by the melting point of the polymer material, these results suggest water is not a suitable heat transfer fluid for most polymeric heat pipes (except those built with high temperature resistant polymers, of course).

Irrespective of the fluid used and of the number of turns of the serpentine channel, the equivalent thermal resistance measured for the horizontal PHP/PHS increases or remains approximately constant when the heating power supply is increased. The evaporator temperature approaches or attains the upper limit imposed by the material already during the second step of the heating
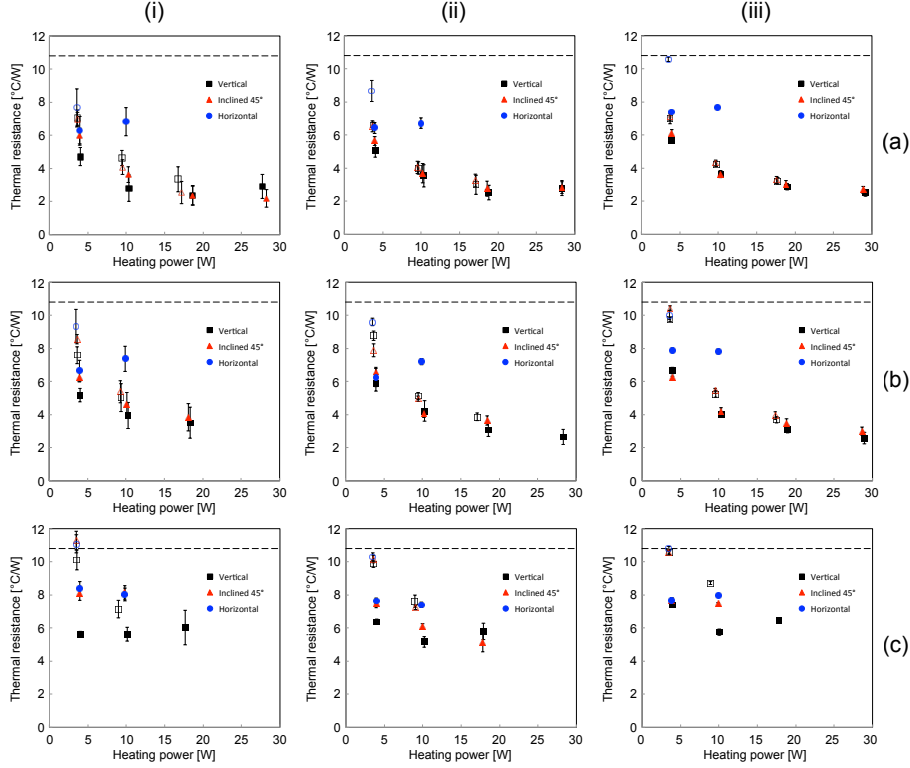
Figure 8: Equivalent thermal resistance of PHP/PHS containing FC-72 (a), ethanol (b), water (c), with a 3-turns (i), 5-turns (ii), and 7-turns (iii) serpentine channel, during an ascending (filled symbols)/descending (open symbols) stepped heating power ramp supplied to the evaporator. The discontinuous horizontal line corresponds to the equivalent thermal resistance of the device without heat transfer fluid. Error bars represent the root mean squared standard deviations of the four temperature measurements, respectively at the evaporator and at the condenser.

power ramp ($\approx$ 10 W). During the descending step, the equivalent thermal re-
sistance often attains the value measured in the absence of heat transfer fluid
because of the relatively large thermal inertia of the system. This suggests the
capillary forces are not sufficiently large to drive the condensate back to the
evaporator, reducing significantly the circulation of the liquid-vapour mixture
hence the heat transfer performance.

These results are in contrast with the standard design guidelines discussed
discussed in Section 2 above, which prescribe the upper and lower limits for
the Bond number to ensure the capillary-driven circulation of the liquid in
the serpentine channel ($0.4 < Bo < 4$). In particular, if the Bond number is
calculated as $Bo = g(\rho_l - \rho_v)D_H^2/\sigma$, the capillary-driven circulation of FC-72
and ethanol should be possible in a channel having a width of 5 mm (Figure 1a),
while if the Bond number is calculated as $Bo = g(\rho_l - \rho_v)D_H^2/\sigma \cos\theta$ to account

14

for wettability, its magnitude falls within the range of PHP operation for all the three fluids considered (Figure 1b). However, the results displayed in Figure 8 suggest none of the fluids considered are suitable to ensure the correct operation of the device when the condensate circulation is not assisted by gravity.

Although the cause of this anomalous behaviour cannot be identified unambiguously at present, one can pinpoint a number of possible mechanisms that can hamper the condensate circulation. Firstly, geometric design parameters such as the length of the channel sections connecting the evaporator and the condenser (≈ 200 mm in this case), and the relativey large aspect ratio of the channel cross-section, which in this case was 1:7, have a direct influence on the frictional losses. An additional factor that may affect the capillary-driven circulation of the liquid is the possible entrapment of the condensate in the dead volume between the serpentine channel and the fittings with the micro-metering valve and the pressure transducer. In any case, one should bear in mind that the limits on the Bond number were established on the basis of boiling and condensation experiments in channels made of high surface energy materials (metals) at relatively high heat fluxes, while the number of studies about boiling and condensation in channels made of low surface energy materials (such as polymers) at low heat fluxes is not significant. This requires further investigation, which may potentially lead to identify an alternative range of Bond numbers applicable to polymeric channels.
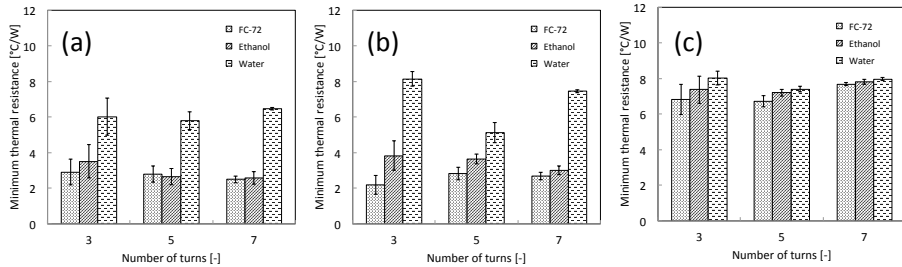

Figure 9: Effect of the heat transfer fluid in a PHP/PHS with vertical (a), inclined at 45° (b), and horizontal (c) orientation.

Figures 9-11 display the minimum equivalent thermal resistance of PHP/PHS, defined here as the equivalent thermal resistance measured at the maximum thermal power supply (about 30 W in the case of ethanol and FC-72, and about 20 W in the case of water) for a given set of design parameters (number of turns, type of heat transfer fluid, and inclination with respect to the horizontal). This quantity is representative of the overall performance of the device, therefore it can be used to compare devices having different design parameters.

The effect of the heat transfer fluid used (FC-72, ethanol or water) is displayed in Figure 9, for different orientations of the PHP/PHS with respect to gravity. In most cases, one can observe a systematic effect of the heat transfer fluid, and the lowest equivalent thermal resistance is achieved in devices containing FC-72, with ethanol closely following. The absolute minimum thermal
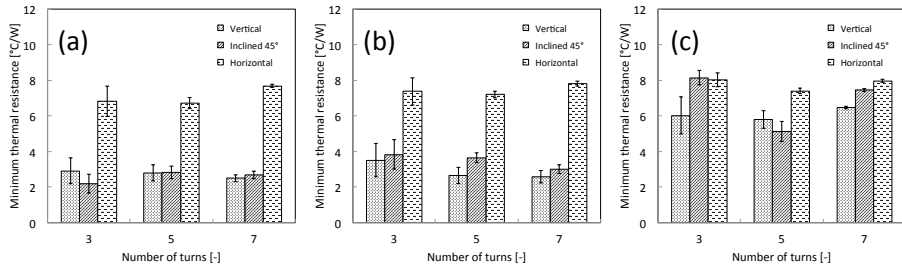
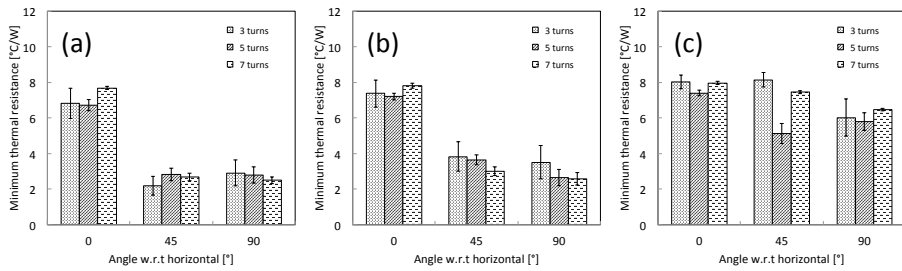Figure 10: Effect of orientation on a PHP/PHS filled with FC-72 (a), ethanol (b), and water (c).

Figure 11: Effect of the number of turns of the serpentine channel on a PHP/PHS filled with FC-72 (a), ethanol (b), and water (c).

resistance measured in this set of experiments is just above 2 °C/W, which represents an increase of the equivalent thermal conductivity with respect to a polypropylene sheet with the same composition and size of 500%.

Figure 10 shows the effect of the PHP/PHS orientation with respect to gravity, for different heat transfer fluids. For FC-72 and ethanol (Figures 10a and 10b), there is a clear performance gap between the vertical or inclined orientations and the horizontal orientation, which confirms gravity is necessary to assist the fluid circulation as discussed above. The equivalent thermal resistances of the pulsating heat pipes inclined of 45° and 90° with respect to the horizontal are comparable with each other, and their difference is within the experimental error, which can be significant because each test was conducted with a fresh PHP.

Finally, the effect of loop geometry (i.e., the number of turns of the serpentine channel) on the PHP/PHS performance is shown in Figure 11. In all cases, there seems to be no significant effect of the number of turns, with the exception of the PHP/PHS containing ethanol with vertical and inclined orientations (Figure 11b), where one can observe a modest but systematic reduction of the minimum equivalent thermal resistance as the number of turns increases.

5. Conclusions

The thermal performance of a polypropylene flat pulsating heat pipe (or "pulsating heat stripes") was investigated experimentally to better understand the effects of three design parameters: the heat transfer fluid, the orientation with respect to gravity, and the number of turns of the serpentine channel, respectively.

In polymeric pulsating heat pipes, where temperatures and the thermal power supply are limited by the relatively low maximum continuous service temperature of the material, usually in the range 100°C-150°C, the phase transition heat and the boiling point of the fluid are the most critical thermophysical parameters, because if they are too large they prevent the heat pipe startup. The contact angle of the fluid on the polymer material and its dependence on temperature are also important because they affect the Bond number; in particular, a large contact angle indicates a poor wettability, which hampers the self-driven capillary flow from the condenser to the evaporator. Thus, fluids with a large latent heat and poor wettability on polymer materials such as water are not suitable heat transfer fluids in this application. Significantly better performances can be obtained using heat transfer fluids having a low latent heat, such as ethanol or perfluorohexane FC-72. In this case, the equivalent thermal conductance of the device can increase up to five times in comparison with that of a polypropylene sheet of the same dimensions.

Irrespective of the heat transfer fluid used, gravity plays a major role in driving the fluid circulation in the serpentine channel, despite the hydraulic diameter was selected so that the Bond number falls within the range commonly prescribed to ensure capillary-driven fluid circulation. This aspects remains ill understood and requires further investigation.

References

References

[1] P. Ruch, T. Brunschwiler, W. Escher, S. Paredes, B. Michel, Toward five-dimensional scaling: How density improves efficiency in future computers, IBM Journal of Research and Development 55 (5) (2011) 15:1–15:13. `doi: 10.1147/JRD.2011.2165677`.

17

[2] L. L. Vasiliev, Heat pipes in modern heat exchangers, Applied Thermal Engineering 25 (2005) 1–19.

[3] H. Ma, Oscillating Heat Pipes, Springer, New York, 2015.

[4] S. Das, V. Nikolayev, F. Lefevre, B. Pottier, S. Khandekar, J. Bonjour, Thermally induced two-phase oscillating flow inside a capillary tube, International Journal of Heat and Mass Transfer 53 (19) (2010) 3905 – 3913. doi:https://doi.org/10.1016/j.ijheatmasstransfer.2010.05.009. URL http://www.sciencedirect.com/science/article/pii/S0017931010002437

[5] M. J. Nine, M. R. Tanshen, B. Munkhbayar, H. Chung, H. Jeong, Analysis of pressure fluctuations to evaluate thermal performance of oscillating heat pipe, Energy 70 (2014) 135 – 142. doi:https://doi.org/10.1016/j.energy.2014.03.098. URL http://www.sciencedirect.com/science/article/pii/S0360544214003624

[6] H. Yang, S. Khandekar, M. Groll, Operational limit of closed loop pulsating heat pipes, Applied Thermal Engineering 28 (1) (2008) 49 – 59. doi:https://doi.org/10.1016/j.applthermaleng.2007.01.033. URL http://www.sciencedirect.com/science/article/pii/S1359431107000683

[7] O. Der, V. Bertola, M. Marengo, A low cost, flexible pulsating heat pipe technology, in: 3rd Thermal and Fluids Engineering Conference (TFEC), no. TFEC-2018-21455, 2018.

[8] O. Der, M. Marengo, V. Bertola, Thermal Performance of Pulsating Heat Stripes Built With Plastic Materials, Journal of Heat Transfer 141 (9), 091808. arXiv:https://asmedigitalcollection.asme.org/heattransfer/article-pdf/141/9/091808/6418956/ht_141_09_091808.pdf, doi:10.1115/1.4041952. URL https://doi.org/10.1115/1.4041952

[9] H. Potente, O. Karger, G. Fiegler, Laser and microwave welding - the applicability of new process principles, Macromolecular Materials and Engineering 287(11) (2002) 734–744. doi:10.1002/mame.200290002.

[10] A. Humbe, P. Deshmukh, C. Jadhav, S. Wadgane, Review of laser plastic welding process, International Journal of Research in Engineering Technology.

[11] O. Der, M. Marengo, V. Bertola, Pulsating heat stripes: A composite polymer sheet with enhanced thermal conductivity, in: Proc. 16th UK Heat Transfer Conference (UKHTC2019), no. UKHTC2019-082, 2019.

[12] O. Der, S. Edwardson, M. Marengo, V. Bertola, Engineered composite polymer sheets with enhanced thermal conductivity, IOP Conference Proceedings: Materials Science and Engineering 613 (2019) 012008.

[13] J. Lim, S. J. Kim, Fabrication and experimental evaluation of a polymer-based flexible pulsating heat pipe, Energy Conversion and Management 156 (2018) 358 – 364. `doi:https://doi.org/10.1016/j.enconman.2017.11.022`.
URL `http://www.sciencedirect.com/science/article/pii/S019689041731066X`

[14] Y. Zhang, A. Faghri, Advances and unsolved issues in pulsating heat pipes, Heat Transfer Engineering 29 (1) (2008) 20–44. `arXiv:https://doi.org/10.1080/01457630701677114`, `doi:10.1080/01457630701677114`.
URL `https://doi.org/10.1080/01457630701677114`

[15] M. Mameli, M. Marengo, S. Khandekar, Local heat transfer measurement and thermo-fluid characterization of a pulsating heat pipe, International Journal of Thermal Sciences 75 (2014) 140–152.

[16] G. B. Wallis, One-dimensional Two-phase Flow, McGraw Hill, 1969.

[17] G. B. Wallis, S. Makkenchery, The Hanging Film Phenomenon in Vertical Annular Two-Phase Flow, Journal of Fluids Engineering 96 (3) (1974) 297–298. `arXiv:https://asmedigitalcollection.asme.org/fluidsengineering/article-pdf/96/3/297/5523701/297\_1.pdf`, `doi:10.1115/1.3447155`.
URL `https://doi.org/10.1115/1.3447155`

[18] I. Chernobylskii, I. Tananaiko, Heat exchange during boiling of liquids in narrow annular tubes, Soviet Phys. Tech. Phys. 1 (10) (1956) 2244–2249.

[19] E. Ishibashi, K. Nishikawa, Saturated boiling heat transfer in narrow spaces, International Journal of Heat and Mass Transfer 12 (8) (1969) 863–893. `doi:https://doi.org/10.1016/0017-9310(69)90153-7`.
URL `http://www.sciencedirect.com/science/article/pii/0017931069901537`

[20] D. Bondurant, J. Westwater, Performance of transverse fins for boiling heat transfer, Chem. Engng Prog. Symp. Ser. 67 (113) (1971) 30–37.

[21] P. A. Kew, K. Cornwell, Correlations for the prediction of boiling heat transfer in small-diameter channels, Applied Thermal Engineering 17 (8) (1997) 705 – 715. `doi:https://doi.org/10.1016/S1359-4311(96)00071-3`.
URL `http://www.sciencedirect.com/science/article/pii/S1359431196000713`

[22] M. Marengo, V. S. Nikolayev, Pulsating Heat Pipes: Experimental Analysis, Design and Applications, Vol. 1, World Scientific, 2018, Ch. 1, pp. 1–62. `arXiv:https://www.worldscientific.com/doi/pdf/10.1142/9789813234406_0001`, `doi:10.1142/9789813234406_0001`.
URL `https://www.worldscientific.com/doi/abs/10.1142/9789813234406_0001`

[23] B. S. Taft, A. D. Williams, B. L. Drolen, Review of pulsating heat pipe working fluid selection, Journal of Thermophysics and Heat Transfer 26 (4) (2012) 651–656. `arXiv:https://doi.org/10.2514/1.T3768`, `doi:10.2514/1.T3768`.
URL `https://doi.org/10.2514/1.T3768`

[24] D. Biolè, V. Bertola, A goniometric mask to measure contact angles from digital images of liquid drops, Colloids and Surfaces A: Physicochemical and Engineering Aspects 467 (2015) 149–156.

[25] D. Biolè, M. Wang, V. Bertola, Assessment of direct image processing methods to measure the apparent contact angle of liquid drops, Experimental Thermal and Fluid Science 76 (2016) 296–305.

[26] J. Israelachvili, Intramolecular and Surface Forces, 3rd Ed., Academic Press, 2011.

[27] L. C. Ruspini, C. P. Marcel, A. Clausse, Two-phase flow instabilities: A review, International Journal of Heat and Mass Transfer 71 (2014) 521 – 548. `doi:https://doi.org/10.1016/j.ijheatmasstransfer.2013.12.047`.
URL `http://www.sciencedirect.com/science/article/pii/S0017931013010922`